Reduced free carrier absorption loss in midinfrared double heterostructure diode lasers grown by liquid phase epitaxy

M. Yin, A. Krier,[a)] R. Jones, and P. J. Carrington
Department of Physics, Lancaster University, Lancaster, LA1 4YB, United Kingdom

An improved InAsSb/InAsSbP double heterojunction ridge laser was designed and grown by liquid phase epitaxy. The cladding layer absorption loss was minimized by the introduction of two undoped quaternary layers on either side of the active region to form a five layer epitaxial structure. The inserted layers also helped alleviate interdiffusion of unwanted dopants into the active region and reduced current leakage in the device. The resulting diode lasers operate readily in pulsed mode near 3.5 μm at elevated temperatures and with a threshold current density as low as 118 A cm^{-2} at 85 K. Compared to the conventional three-layer double heterostructure laser, the modified structure with reduced optical loss increased the maximum lasing temperature by 95–210 K. © *2007 American Institute of Physics*. [DOI: 10.1063/1.2779246]

There is increasing interest in the development of mid-infrared (2–5 μm) diode laser sources for applications in molecular spectroscopy, optical gas sensors, and free space optical communications. To access room temperature operation within this technologically difficult spectral range, several different device designs are being developed, including unipolar quantum cascade lasers[1] and interband cascade lasers (ICLs) based on "W" structures.[2–4] However, although promising, these devices contain many ultrathin layers (there are 3000 interfaces in ICL structures) and the fluctuation in composition, uncertainties in material quality and heterojunction roughness, waveguide fabrication, etc., are difficult to control in manufacture.[5,6] The cascade lasers also have higher operating voltages than those of conventional bipolar diode lasers. In this work we demonstrate midinfrared diode lasers with improved performance fabricated using a much simpler approach based on liquid phase epitaxy (LPE). We report specifically on a five-layer double heterojunction (DH) laser with reduced optical loss emitting at 3.45 μm and operating up to 210 K.

LPE is a near equilibrium growth technique which produces epitaxial layers of high crystalline perfection containing few point defects and impurities. The relatively high growth rate ($\sim$1 μm/min) is useful for the production of the cladding layers or broad waveguide regions in a high power diode laser. In addition, LPE growth also has the potential for cost effective device manufacture. For conventional DH diode lasers, a maximum operating temperature of 150 K (with 6 W output at 78 K) has been achieved.[7,8] To obtain higher operating temperatures and lower threshold current, it is necessary to reduce the Auger coefficient and free carrier leakage. The crucial role of internal loss (α_i) in limiting both the differential quantum efficiency (η_d) and maximum operating temperature has been realized.[9,10] The doping induced absorption loss for InAs related alloys at wavelengths around 3.4 μm can be as high as 200 cm^{-1}.[11] Therefore, it is also important to minimize the optical loss originating from the highly doped cladding layers. Our laser design is based on the InAs$_{1-x}$Sb$_x$/InAs$_{1-x-y}$Sb$_x$P$_y$ DH alloy system, from which wavelengths covering most of the midinfrared spectral range

can be accessed through the adjustment of the alloy compositions. In the conventional DH laser structure, the InAs$_{1-x}$Sb$_x$ active region is sandwiched between two InAs$_{1-x-y}$Sb$_x$P$_y$ cladding layers. Some of the optical mode overlaps with the highly doped cladding layers, which introduces optical loss due to free carrier absorption, as shown in Fig. 1(a). In our structure, undoped InAs$_{0.61}$Sb$_{0.13}$P$_{0.26}$ layers are inserted between the heavily doped InAs$_{0.61}$Sb$_{0.13}$P$_{0.26}$ cladding layers on either side of the InAs$_{0.96}$Sb$_{0.04}$ active region, as shown in Fig. 1(b), in an attempt to reduce the optical mode overlap with the heavily doped layers. The undoped layers also block unwanted impurity diffusion into the laser active region and give improved carrier confinement.

The active region composition of InAs$_{0.96}$Sb$_{0.04}$ was selected to emit within the atmospheric transmission window at the wavelength of 3.7 μm at room temperature. Figure 1 shows the calculated fundamental TE mode profiles for the conventional and five-layer DH structures, where the thicknesses of the InAs$_{0.96}$Sb$_{0.04}$ active region and InAs$_{0.61}$Sb$_{0.13}$P$_{0.26}$ cladding layers were 0.8 and 2.0 μm, re-
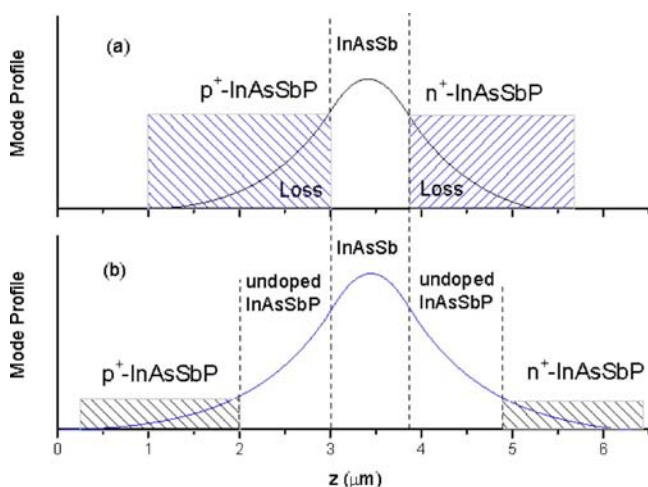

FIG. 1. (Color online) InAs$_{0.61}$Sb$_{0.13}$P$_{0.26}$/InAs$_{0.96}$Sb$_{0.04}$ fundamental TE optical mode profile along the growth axis for (a) conventional three-layer DH laser and (b) five-layer DH structure with additional undoped InAs$_{0.61}$Sb$_{0.13}$P$_{0.26}$ layers inserted between the InAsSb active region and the highly doped InAsSbP cladding layers.
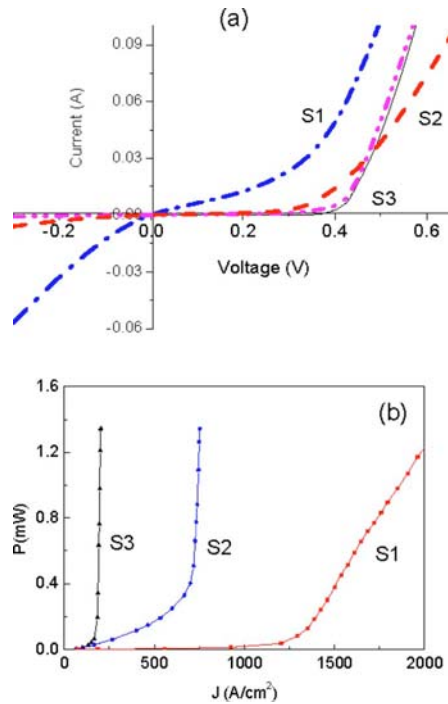
---

a)Electronic mail: a.krier@lancaster.ac.uk

FIG. 2. (Color online) (a) Current-voltage and (b) light-current relationships for the three different samples at the temperature of 100 K, where "thin" represents 2×0.25 μm inserted undoped epilayers (S2) and "thick" represents 2×1 μm inserted undoped epilayers (S3) in the device. *P* is the output power measured from both facets.

spectively. The thickness of the undoped InAsSbP layers was selected to be (S1) 0 μm, (S2) 0.25 μm, and (S3) 1.0 μm in the lasers which were subsequently fabricated. The fundamental transverse TE mode profile confinement factor (Γ) was calculated as 35% for the conventional three-layer DH laser structure in Fig. 1(a). In this case 65% of the mode overlaps the highly doped cladding layers, which contributes significantly to the total optical loss in the device. In the five-layer DH structure of Fig. 1(b) the confinement factor is nearly the same (32%) as that in the active region. However, the transverse mode overlap with the highly doped cladding layers is considerably decreased to 20%, due to the insertion of the undoped layers.

The DH structures were grown onto (100) oriented *p*-type InAs substrates from indium-rich melts using a conventional multiwell graphite sliding boat and epitaxial growth technique which has been developed and described previously.[12] The cladding layers were intentionally doped with Te (*n* type) up to a concentration of 5×10^{18} cm^{-3} and with Zn (*p* type) up to 1×10^{18} cm^{-3}, respectively. The thickness of each epilayer was measured by scanning electron microscopy on cross-sections which were stained using the *A*:*B* etch. The epilayer compositions were determined using both energy-dispersive x-ray analysis and double crystal x-ray diffraction measurements.

Edge emitting ridge laser structures were fabricated from the epitaxial wafers using conventional photolithography and wet chemical etching to produce ridges which were 0.5 μm deep and 50 μm wide. RF sputtering was used to deposit the SiO$_2$ which was used as an insulating layer. Ohmic contacts were formed by thermal evaporation of Au:Zn and Au:Te alloys at 150 °C on the *p* and *n* sides of the structures, respectively. Laser chips were mounted *n*-side (epilayer side)
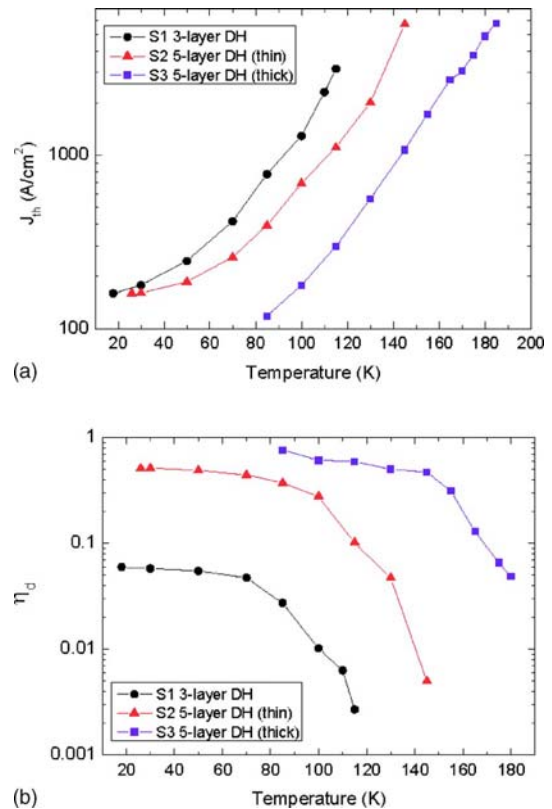

FIG. 3. (Color online) (a) Dependence of threshold current density (J_{th}) on temperature (*T*) and (b) the dependence of differential quantum efficiency on temperature for the samples S1, S2, and S3.

up onto TO-49 headers for testing. The spontaneous electroluminescence emission from sample S3 gave a peak at 3.70 ± 0.02 μm at room temperature. Current-voltage-light (*I*-*V*-*L*) characteristics were measured at different temperatures for the different DH laser samples S1, S2, and S3 respectively. Figure 2 shows current-voltage (*I*-*V*) and light-current (*L*-*I*) curves at 100 K for conventional three-layer and two different five-layer DH laser structures, each with a cavity length of 500 μm. The *L*-*I* relationships were obtained under pulsed conditions using a pulse width of 100 ns and a frequency of 100 Hz.

From the *I*-*V* curves in Fig. 2(a), sample S3 (1.0 μm thick insertion layers) exhibits the least forward and reverse leakage current associated with improved confinement and reduced impurity inter-diffusion. The calculated *I*-*V* curve is represented by the solid line and is in excellent agreement with the experimental data for S3. From Fig. 2(b), it is evident that the introduction of two thin layers (S2) reduces the threshold current density and increases the efficiency at the same operating temperature. Increasing the thickness of the undoped insertion layers produces further improvements as is evident from the curve for S3.

The experimental results in Fig. 3 show the temperature dependence of the different lasers. Sample S3 has the lowest threshold current density ($J_{\text{th}}=118$ A cm^{-2} at 85 K), the highest laser differential quantum efficiency ($\eta_d=76\%$ at 85 K), slowest efficiency degradation ($\sim$2.4 times from 85 to 155 K, compared to approximately ten times from 75 to 150 K in Ref. 7), and almost constant characteristic temperature T_0 over a wide temperature range ($T_0=24$ K from 85 to 185 K), due to the insertion of the two 1 μm

TABLE I. Comparison of the five-layer DH laser (S3) with some midinfrared lasers of similar construction at wavelengths of 3.3–3.5 μm at temperatures of 80–100 K.

	J_{th} (A cm^{-2})	η_d (%)	α_i (cm^{-1})	η_i
Present work S3 (100 K)	177	61	12	0.93
Conventional DH (100 K)[a]		6	42	
Asymmetric DH (80 K)[b]	300	34		
Type-II QW (90 K)[c]	150	30	30	0.67

[a]Reference 12.
[b]Reference 8.
[c]Reference 10.

undoped layers. The internal loss in our lasers (at 100 K) was determined experimentally in the usual manner by measuring the differential efficiency of lasers with different cavity lengths. The loss in sample S1 was ~60 cm^{-1} and is much higher than that of sample S3 which was reduced to 12 cm^{-1}. As shown in Table I, our DH laser (S3) also has higher efficiency and lower loss compared to other similar midinfrared lasers of simple construction.

Some typical measured laser spectra at different temperatures are presented in Fig. 4 for sample S3, where a maximum laser emission wavelength of 3.45 μm was o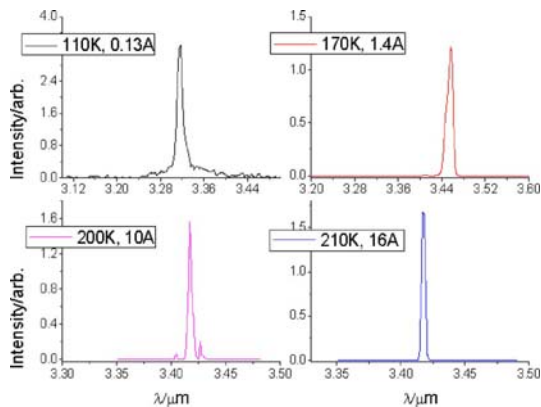btained at 170 K. The maximum temperature of laser operation in pulsed mode was found to be 210 K, which is more than 90 K higher than that of the conventional three-layer DH laser (S1, maximum lasing temperature ~115 K) using the same growth and processing conditions.

In summary, an improved five-layer DH laser structure of relatively simple construction has been fabricated by LPE and characterized. As expected from simulations these midinfrared diode lasers exhibited reduced threshold current (118 A/cm^2 at 85 K), superior efficiency degradation with increasing temperature and a significantly higher maximum operating temperature of 210 K. We attributed this mainly to the addition of the undoped layers which reduced the optical loss to 12 cm^{-1}. Using the same epi-layer growth and device processing conditions, laser operating temperature was increased by 90 K in the five-layer DH structure (S3), compared with the conventional three-layer DH structure (S1). The characteristic temperature $T_0=24$ K for the five-layer DH laser remained constant over a wide temperature range from 85 to 185 K.

FIG. 4. (Color online) Typical laser spectra measured from S3 using different injection currents and temperatures.

[1]J. S. Yu, S. R. Darvish, A. Evans, J. Nguyen, S. Slivken, and M. Razeghi, Appl. Phys. Lett. **88**, 041111 (2006).

[2]C. L. Canedy, W. W. Bewley, M. Kim, C. S. Kim, J. A. Nolde, D. C. Larrabee, J. R. Lindle, I. Vurgaftman, and J. R. Meyer, Appl. Phys. Lett. **90**, 181120 (2007).

[3]C. L. Canedy, W. W. Bewley, J. R. Lindle, C. S. Kim, M. Kim, I. Vurgftman, and J. R. Meyer, J. Electron. Mater. **35**, 453 (2006).

[4]W. W. Bewley, J. R. Lindle, and J. R. Meyer, Appl. Phys. Lett. **81**, 1166 (2002).

[5]A. V. Gopal, H. Yoshida, T. Simoyama, N. Georgiev, T. Mozume, and H. Ishikawa, Appl. Phys. Lett. **80**, 4696 (2002).

[6]R. Teissier, D. Barate, A. Vicet, C. Alibert, A. N. Baranov, X. Marcadet, C. Renard, M. Garcia, C. Sirtori, D. Revin, and J. Cockburn, Appl. Phys. Lett. **85**, 167 (2004).

[7]M. Aydaraliev, N. V. Zotova, S. A. Karandashov, B. A. Matveev, M. A. Remennyi, N. M. Stus, and G. N. Talalakin, Appl. Phys. Lett. **81**, 1166 (2002).

[8]D. Wu, B. Lane, H. Mohseni, J. Diaz, and M. Razeghi, Appl. Phys. Lett. **74**, 1194 (1999).

[9]H. Q. Le, C. H. Lin, S. J. Murray, R. Q. Yang, and S. S. Pei, IEEE J. Quantum Electron. **34**, 1016 (1998).

[10]A. Wilk, M. El Gazouli, M. El Skouri, P. Christol, P. Grech, A. N. Baranov, and A. Joullie, Appl. Phys. Lett. **77**, 2298 (2000).

[11]http://www.ioffe.rssi.ru/SVA/NSM/Semicond/InAs/

[12]A. Krier, H. H. Gao, and V. V. Sherstnev, J. Appl. Phys. **85**, 8419 (1999).